Synthesis and Characterization of Iron-Containing MCM-41 Porous Silica by the Exchange Method of the Template

A. B. Bourlinos, M. A. Karakassides,† and D. Petridis*

Institute of Materials Science, National Center for Scientific Research "Demokritos", 15310 Ag. Paraskevi, Attikis, Athens, Greece

Received: December 9, 1999

The synthesis and characterization of iron-containing MCM-41 porous silica using the exchange method of the template with the iron salts $FeCl_3 \cdot 6H_2O$ and $(Fe_3Ac_6O \cdot 3H_2O)NO_3$ is reported. Proper conditions under which the exchange reactions can be accomplished without destroying the lattice structure of the parent MCM-41 material were examined. Quantitative measurements upon template removal reveal the existence of ion pairs of surfactant molecules as a constituent of the template structure. Mesoporous silica planted with iron exhibits good thermal stability and high surface areas. Reflectance-IR, EPR, and Mössbauer measurements provide clear evidence for the iron grafting into the silicon oxide network of the calcined products.

Introduction

MCM-41 materials belong to a family of products, designated as M41S, discovered by Mobil Oil Co. a few years ago.[1] The as-synthesized materials exhibit a hexagonal arrangement of pores occupied by an organic phase, functioning as a template in the synthesis, while between them there is a partially condensed inorganic oxo-hydroxide silicon network.[2,3]

The kind of interactions between the inorganic network and the template depends upon the synthetic route of the material and is of two types:[4] Coulombic (S^+I^-) and hydrogen bonding ($S^\circ I^\circ$ or $S^+X^-I^+$) [S^+ stands for ionic surfactant, S° for neutral, and I for the inorganic network]. In the latter case the template can be easily removed by hot ethanol, while in the case of Coulombic interactions the presence of an exchange reagent is required.[5] The main difference between the two treatments is that for hydrogen-bonding interactions, network connectivity is high and no collapse of the structure is observed upon template removal, while for the Coulombic interactions case total removal of the template with an exchange cation gives an amorphous product[6] because of smaller network connectivity in the as-synthesized product.[4]

Iron-substituted MCM-41 derivatives have been described in the literature.[7−12] In this paper we report the synthesis of iron-modified MCM-41 materials based on the exchange method of the template[5,6,13,14] and also investigate, using reflectance-IR and X-ray methods, the role of network connectivity in keeping the structural features of the parent MCM-41 material unaltered upon template removal. Finally, the constitution and organization of the template phase in the as-synthesized MCM-41 solid were examined.

Synthesis

Starting Materials. For the synthesis of the MCM-41 material a 50 wt % of an aqueous solution of cetyltrimethylammonioum chloride (C16TMACl) as the template and tetramethoxysilane (TMOS) as the silica source, both supplied from Merck-Schuchardt, were used. For the exchange reactions the following salts were used as the iron sources: $FeCl_3 \cdot 6H_2O$ from Panreac and $(Fe_3Ac_6O \cdot 3H_2O)NO_3$ prepared by a known procedure.[15]

Procedure. *(a) MCM-41 S^+I^- Type.*[16] In a solution of 65.7 g of deionized water and 12.5 g of methanol, 3.6 g of a 50% aqueous solution of C16TMACl was added followed by the addition of 9−12 drops of a 50% sodium hydroxide solution. A solution of 6.5 g of TMOS in 10 g of methanol was added to the template solution. To the white precipitate, formed after a few seconds, 10 mL of ethanol was added and the mixture was stirred at room temperature for 3 h. Finally, the white solid was centrifuged, washed several times (7−8) with water until negative test for chloride ions in the supernatant liquid, and spread on a glass plate for drying. The sample was placed in an oven at 100 °C for 11 days (MCM-41/100). A portion of the dried solid was calcined in air for 2 h at 450 °C in steps of 0.5 °C/min (MCM-41/450).

(b) Fe-MCM-41. 0.8 g of MCM-41/100 solid was dispersed in 30 mL of an ethanolic 0.1 M $FeCl_3 \cdot 6H_2O$ solution. The mixture was transferred to an oil bath and stirred for 3 h at 60 °C. After reaction, the solid was centrifuged and washed very well with water until the supernatant liquid was colorless. Then it was redispersed in ethanol and dried in a glass plate. The sample placed in an oven at 100 °C for 24 h before calcination. 0.47 g of a white solid was obtained (FeMS). A portion of the sample was calcined at 450 °C in air for 2 h in steps of 0.5 °C/min. A white solid (FeMS450) was produced with an iron content of 1.6%.

(c) Fe3-MCM-41. 0.8 g of MCM-41/100 material was dispersed in 30 mL of ethanol containing 0.86 g of the trinuclear iron acetate complex $(Fe_3Ac_6O \cdot 3H_2O)NO_3$. The mixture was stirred for 30 h at room temperature. After washing and drying, 0.58 g of an orange solid was obtained (Fe3MS). A portion of this sample was calcined at 450 °C as above, giving an orange product (Fe3MS450) with an iron content of 2.7%.

(d) Template Isolation. The template was isolated in the form of its perchlorate salt as following:

(i) In the case of simple ethanol treatment, a dried sample of MCM-41/100 was treated for 3 h in hot ethanol (60 °C). After

* To whom correspondence should be addressed.
† Current address: Department of Materials Science and Technology, University of Ioannina, P.O. Box 1186, Ioannina, GR-45110, Greece.

10.1021/jp994328u CCC: $19.00
Published on Web 04/14/2000

solid separation (MCM-41/EtOH), the ethanol solution was condensed and to the condensate a few drops of an aqueous sodium perchlorate solution were added. The white precipitate ($S^+ClO_4^-$) was washed with water and dried at 35 °C for 24 h.

(ii) In the case of iron trichloride treatment, after reaction and solid separation the remaining iron in the washings was first removed in the form of hydrous oxide by adding a few drops of concentrated NH_4OH and then the surfactant was isolated as in the previous case.

A blank experiment showed that precipitation of surfactant with $NaClO_4$ is accomplished to a 85% level.

Structure Characterization. X-ray powder diffraction patterns were recorded on a Siemens XD-500 diffractometer using Cu Kα radiation. The data were collected in the 2θ region 1°−10° with slits 0.3/0.3/0.3/0.15/0.15 and scanning rate 0.03°/s. The IR-reflectance spectra were taken with an FT-IR spectrometer, Bruker, equinox 55/S model, equipped with a specac variable angle attachment. Each spectrum was the average of 100 scans collected at 2 cm^{-1} resolution by means of unpolarized radiation at an incident angle of 20° to normal. The reflectance data were analyzed by Kramers−Krönig inversion to yield the real absorption coefficient spectra of the samples. Electron paramagnetic resonance spectra were recorded at 20 K on a Bruker 200D-SRC spectrometer equipped with an Oxford ESR9 cryostat. A conventional constant acceleration Mössbauer spectrometer with $^{57}Co(Rh)$ source was used to record the spectra. Adsorption isotherms were taken on a nitrogen Autosorb 1 Quantacrome Corp. porosimeter at 77 K. All samples were first degassed in a vacuum prior to analysis. The BET surface areas were calculated in the region 0.05−0.3 of relative pressures while the mean pore diameters were calculated assuming a cylindrical pore model.[17] Iron determination was made by the method of 1,10 phenanthroline[18] using a Shimadzou UV2100 photospectrometer.

Results and Discussion

Network Connectivity. An important factor in the exchange reactions of an as-synthesized MCM-41 material with iron or other metal ions is the network connectivity of the mesoporous structure. By this term we mean the degree of condensation of tertiary Si−OH groups toward bridged Si−O−Si groups. This parameter is important for retaining the structural integrity of the mesoporous material upon template removal, since the latter acts as a pillar in the MCM-41 framework construction. Indeed, when an as-synthesized MCM-41 sample was subjected to an exchange reaction with an iron salt in alcohol before any drying we observed a total collapse of the structure upon template removal, whereas the same reaction applied to a dried sample gave products of high crystallinity (Figure 1).

This behavior can be attributed to an enhanced network connectivity attained during the drying process. The effect of drying on the silicon oxy-hydroxide lattice connectivity can be observed in the absorption coefficient spectra shown in Figure 2. The spectra were derived from the corresponding reflection spectra of the as-synthesized product before (a) and after drying (b). Spectrum (b) compared to (a) shows a decrease in the intensity of the absorption band at 965 cm^{-1} relative to the main peak at 1075 cm^{-1} and also a small shift in the main band from 1068 cm^{-1} to 1075 cm^{-1}. Since the shoulder at 965 cm^{-1} arises from stretching vibrations of the Si−OH bonds and the band at 1075 cm^{-1} from Si−O−Si bonds,[19] the above changes suggest an increment in the Si−O−Si bonds at the expense of Si−OH bonds. Analogous IR changes have been observed when an amorphous gel is calcined to high temperatures whereupon polycondensation reactions mold the SiO_2 network.[19]

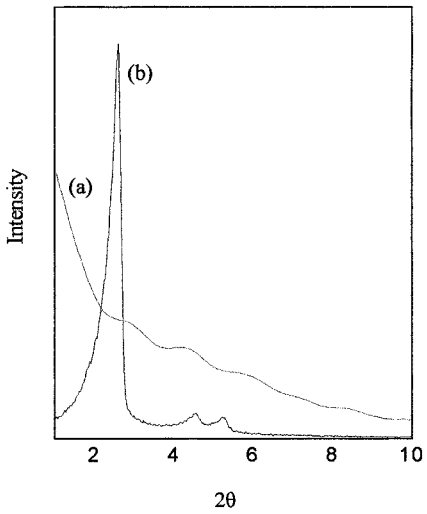

Figure 1. XRD patterns of an as-synthesized sample MCM-41 (a) and dried one (b) after exchange reactions with iron salts.

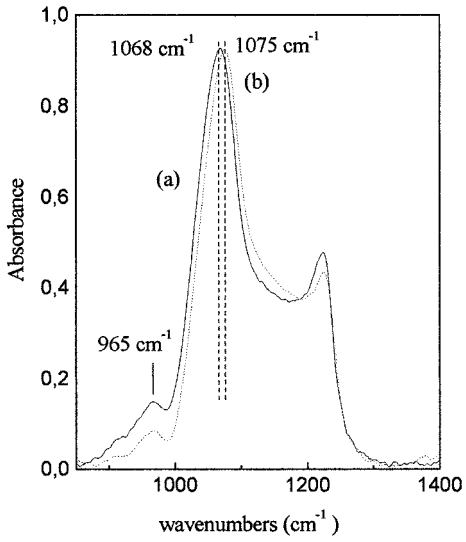

Figure 2. Absorption coefficient spectra of (a) an as-synthesized (solid curve) and (b) dried MCM-41 sample (dot curve).

The IR observations about network connectivity are also supported by the XRD patterns of the same samples (Figure 3). Drying induces a shift in the (100) reflection toward larger 2θ values, reflecting lattice shrinkage, and also loss of the (210) reflection, indicating lower crystallinity. Similar changes, but much more intense, were also noticed for a calcined at 450 °C MCM-41 material (Figure 3c). Calcination in this case causes the maximum network connectivity (Si−O−Si ≫ Si−OH).

Template Isolation. Evidence for the removal of template molecules during exchange reactions with ferric chloride or trinuclear ferric acetate in ethanol comes from a considerable loss in the weight of the starting dried materials and also from a dramatic decrease in the absorption between 3000 and 2800 cm^{-1} of the organic template moieties.

In Table 1 we give the results from quantitative measurements made for the FeMS product. According to the data, treatment of a dried MCM-41/100 sample only with ethanol (60 °C, 3 h) leads to a weight loss which is the same as that from an as-synthesized product without drying. We attribute this loss to the presence in the template structure of ion pairs S^+X^- that interact weakly via hydrogen bonding with free hydroxyl groups of the inorganic network (Si−OH X^-S^+). Leaching of these

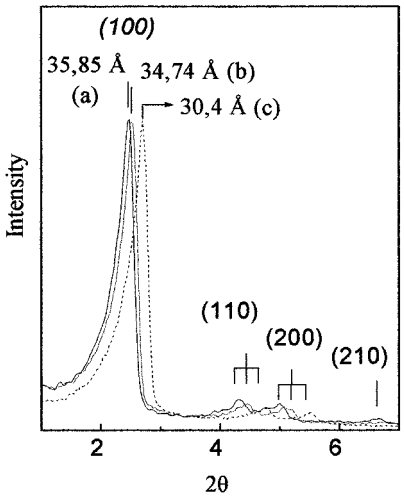

Figure 3. XRD patterns of an MCM-41 sample before (a) and after drying process (b) and calcined at 450 °C (c).

ion pairs by the ethanol treatment is also supported by a decrease in the intensities of absorptions from vibration of the organic moieties.

In order to further demonstrate the presence of ion pairs, portions of ethanol-treated and non-ethanol-treated samples were dispersed in aqueous solutions of $K_4[Fe(CN)_6]$. The resulting products were washed well with water, dried and then characterized by IR spectroscopy (Figure 4). The non-ethanol-treated solid shows a characteristic band at 2027 cm^{-1} due to stretching vibrations of cyanide ligands. The appearance of this band results from the replacement of halide ions by $Fe(CN)_6^{4-}$ according to the reaction:

$$4S^+X^- + Fe(CN)_6^{4-} \rightarrow S_4Fe(CN)_6 + 4X^-$$

On the contrary, the ethanol-treated solid did not exhibit any cyanide absorption at 2027 cm^{-1}.

Treatment of a dried MCM-41 material with an ethanolic iron chloride solution causes a weight loss not only from the removal of ion pairs but also from surfactant cations S^+ that are electrostatically bound to the negatively charged oxygens of the inorganic network. This latter surfactant removal is accomplished via the following cation exchange reaction:

$$3Si{-}O^-S^+ + Fe^{3+} \rightarrow (Si{-}O^-)_3Fe^{3+} + 3S^+$$

In general, when weight loss occurred, we could isolate the released surfactant molecules in the form of the perchlorate salt. From the data in Table 1, we conclude that there is a good agreement between calculated perchlorate salt formation assuming 100% yield of precipitation and those measured quantitatively with a precipitation yield 85%. In addition, based on the total organic phase weight of the starting material, calculated from the weight difference between the as-synthesized and calcined to 500 °C[13] MCM-41 material, we can estimate the efficiency of the template removal. This equals to 0.040/0.043 × 100 or 93%. As far as the contribution of ion pairs (S^+X^-) to the template structure ($S^+I^- + S^+X^-$) is concerned, this is found to be equal to 0.014/0.043 × 100 or 33%.

We must notice that in the case of the FeMS product the weight loss is larger than for the Fe3MS case, although both samples exhibit efficient template removal as indicated by the IR spectra. We believe that this difference arises from the different ferric units inserted to the MCM-41 framework. In the case of FeMS we have the insertion of simple iron cations, while in the case of Fe3MS heavier trinuclear oxo iron moieties are inserted, the exact form of which (number of acetate substituents) cannot be predicted because of probable hydrolysis. Furthermore, comparison of the IR spectrum of the Fe3MS product to that of iron triacetate complex does not reveal similarities from the acetate groups. This indicates a partial destruction of the acetate ligands during the exchange reaction leading to a hydrolyzed oligonuclear acetato complex which is more favorably adsorbed by the anionic exchange sites.

Iron Grafting. Figure 5 presents the XRD patterns of Fe-MCM-41 and Fe3-MCM-41 before and after calcination at 450 °C. For comparison we include the XRD pattern of an MCM-41 sample calcined at 450 °C under the same conditions (MCM-41/450). A marker for iron grafting into the silicate network comes from an increase in the lattice parameter a_o or equally in the d_{100} spacing ($a_o = 2/\sqrt{3}d_{100}$) relative to that of an MCM-41/450 sample. This increase can be accounted for by the insertion of the larger Fe^{3+} cations (radius 0.65 Å vs 0.26 Å for Si^{4+}) in the silicate network. The parameter d_{100} is 33.7 Å for FeMS450 and 30.4 Å for MCM-41/450. The same holds also for the Fe3MS450 solid (31.1 Å against 30.4 Å).

Iron grafting is also registered by the absorption coefficient spectra in Figure 6. We observe that the iron-containing solids exhibit a small shift in the main absorbance band from the Si−O−Si vibration from 1098 cm^{-1} for the MCM-41/450 sample to 1093 cm^{-1}. This shift, even small, is in line with the existence of Si−O−Fe moieties expected to occur at lower frequencies as a consequence of their greater reduced mass.

In order to evaluate the wall thickness π of the iron-planted solids as well as the BET surface area and the mean pore radius, we present in Figure 7 their adsorption isotherms and that of MCM-41/450 sample. The shapes are characteristic for porous materials with a hexagonal pore arrangement while the steep slops are indicative of high crystallinity products. The BET surface areas for the FeMS and Fe3MS solids were 1127 and 750 $m^2\ g^{-1}$, respectively. The data reflect template removal since an as-synthesized MCM-41 material possesses external surface of only 47 $m^2\ g^{-1}$ because of pore occupancy by template molecules.

Table 2 presents results from the XRD and adsorption isotherms data analysis. The data show that the materials FeMS450 and Fe3MS450 are microporous ($d_\pi \sim 14$ Å), of large surface area and increased wall thickness as compared to an MCM-41/450 sample. Porous solids with enhanced wall thickness are attractive for high-temperature catalytic reactions.

Figure 8 presents the EPR spectra recorded at 20 K of the iron-containing samples before and after calcination and that of pure iron triacetate complex, the structure of which is known.[20] Signals at $g \sim 4.3$ and $g \sim 2.0$, although still a matter of debate, are typical for iron grafting in an environment of a distorted cubic symmetry.[8] A careful examination of the calcined samples spectra reveals that the bandwidth of the signal at $g \sim 4.3$ is larger for the Fe3MS450 sample than that of FeMS450. This difference arises probably from the different structure of the inserted iron species. The close proximity of the iron centers in the partially hydrolyzed acetate complex entails a shorter spin−spin relaxation time and therefore broader signals for the Fe3MS450 sample. In addition, the higher intensity of the signal at $g \sim 2.3$ can be attributed to the higher level of iron centers in the Fe3MS450 compared to FeMS450. These results were essentially the same regardless whether the calcined samples were measured shortly after the calcination process or after their rehydration by exposing in air.

As was previously stated, during the exchange reaction in

TABLE 1: Quantitative Measurements upon Template Removal

dried samples	wt (g)	weight diff	assignment	expected $S^+ClO_4^-$ quantity (100%)	measd quantity (85%)	observable yields (%)
MCM-41/100	0.096					
MCM-41/EtOH	0.082	0.014	S^+X^-	0.0168	0.014	83.3
FeMS	0.056	0.040	$S^+X^- + S^+$	0.052	0.044	84.5
MCM-41/500	0.053	0.043	template's combustion			

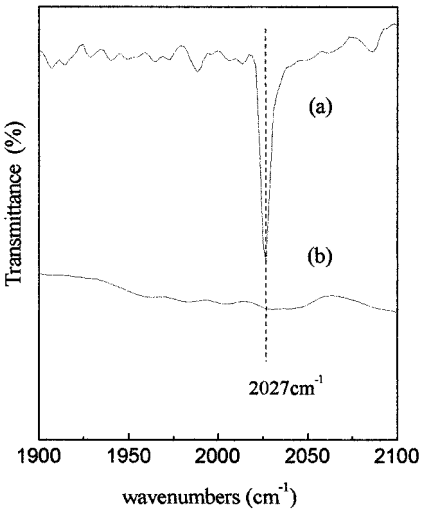

Figure 4. IR spectra of (a) MCM-41 and (b) MCM-41/EtOH after treatment with the $K_4[Fe(CN)_6]$ salt.

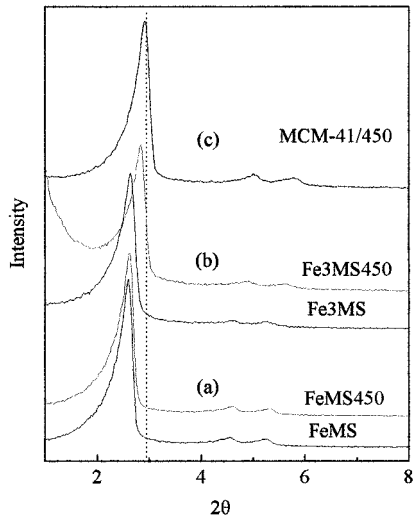

Figure 5. XRD patterns of samples (a) FeMS (lower) and FeMS450 (upper), (b) Fe3MS and Fe3MS450, and (c) MCM-41/450.

the MCM-41/100−iron triacetate system with the iron acetate complex, a partial destruction of acetate groups occurs. This finding is also supported by the different EPR spectra of the iron complex and that of Fe3MS sample. In the pure iron complex the EPR spectrum exhibits a relative broad signal at $g \sim 4.96$, attributable to a pseudo-octahedral coordination symmetry around iron centers, while for the Fe3MS sample the g value changes to 4.3, suggesting the presence of iron centers in a different environment than in the trinuclear acetate complex.

Strong evidence for iron grafting into the silicon oxide matrix comes from the ^{57}Fe Mössbauer spectra of the samples FeMS450 and Fe3MS450 recorded at room temperature and at liquid nitrogen (Figure 9). The main characteristic of the spectra is the presence of a quadrapole doublet due to a distorted cubic symmetry around iron centers, while the isomer shift values (0.2−0.4 m s^{-1}) are indicative for trivalent oxidation state of

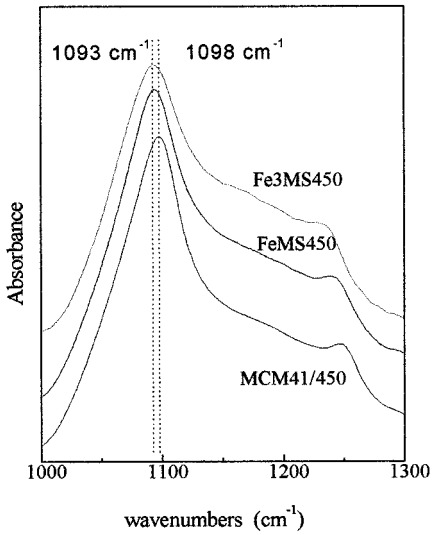

Figure 6. Absorption coefficient spectra of samples FeMS450, Fe3MS450, and MCM-41/450.

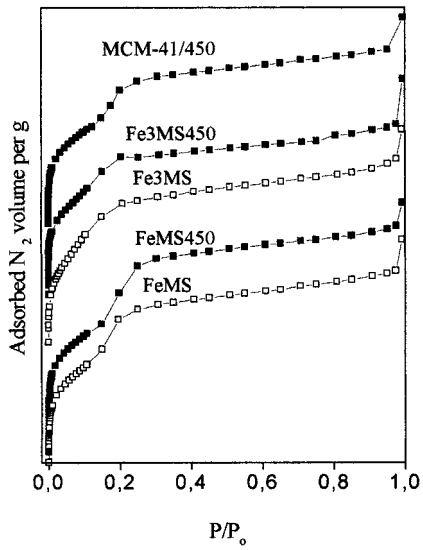

Figure 7. Adsorption isotherms of iron-containing samples before (open squares) and after calcination (solid squares) and that of the calcined sample MCM-41/450.

TABLE 2: Structural Properties of Samples Fe-MCM-41 and Fe3-MCM-41 before and after Calcination at 450 °C

sample	d_{100} (Å)	a_o (Å)	r_p (Å)	π (Å)	S_{BET} (m^2 g^{-1})
FeMS	33.9	39.14	7.0	25.14	1127
FeMS450	33.7	38.91	7.0	24.91	1264
Fe3MS	33.5	38.68	7.5	23.68	750
Fe3MS450	31.1	35.91	6.5	22.91	915
MCM-41/450	30.4	35.10	8.5	18.10	1021

the iron atoms.[21] Isomer shift (δ) and quadrapole splitting (Δ) values measured at different temperatures are listed in Table 3. We observe that the δ values increase with decreasing the temperature for both samples FeMS450 and Fe3MS450, while the parameter Δ remains practically constant. These observations

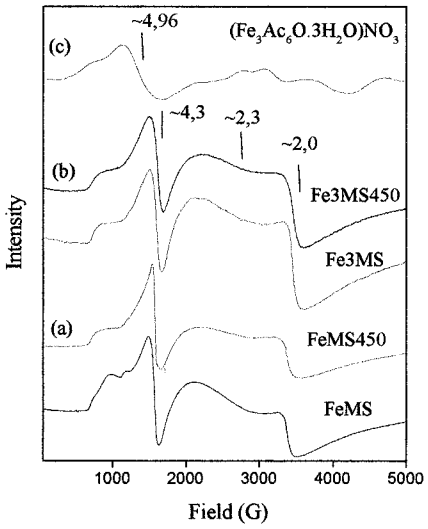

Figure 8. EPR spectra of samples (a) FeMS (lower) and FeMS450 (upper), (b) Fe3MS and Fe3MS450, and (c) $(Fe_3Ac_6O{\cdot}3H_2O)NO_3$ recorded at 20 K.

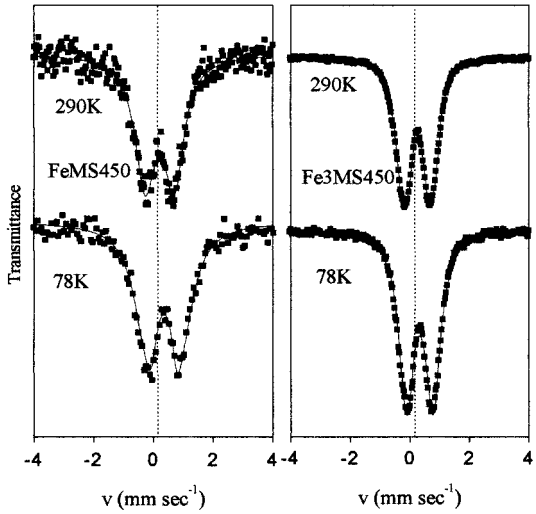

Figure 9. Mössbauer spectra of samples FeMS450 and Fe3MS450, recorded at both room temperature and liquid nitrogen.

TABLE 3: Results of the Mössbauer Measurements over the Calcined Iron Containing Samples

sample	δ (mm s^{-1})	Δ (mm s^{-1})
FeMS450/290 K	0.209	0.936
FeMS450/78 K	0.371	0.945
Fe3MS450/290 K	0.260	0.877
Fe3MS450/78 K	0.335	0.888

are in accordance with what has been reported for ferric zeolites[22] and offer additional evidence for iron grafting. Furthermore, in order to decide about the nature of the iron species in the materials, both samples FeMS450 and Fe3MS450 were also measured at liquid He temperature. The spectra (not shown) revealed no splitting of the central paramagnetic doublet line into a sextet, indicating the absence of any nano iron oxide phases in the materials[12,22] without excluding the possibility for the presence of oligonuclear iron clusters (2−3 iron atoms), especially in the case of Fe3MS450 sample.

Accessibility and Stability of Iron Centers. An important question concerns the accessibility of the iron centers by molecules adsorbed to the pores of the iron modified MCM-41 materials. To test this possibility, both FeMS450 and Fe3MS450 were exposed to vapors of acetic anhydride for 2 h at 60 °C.

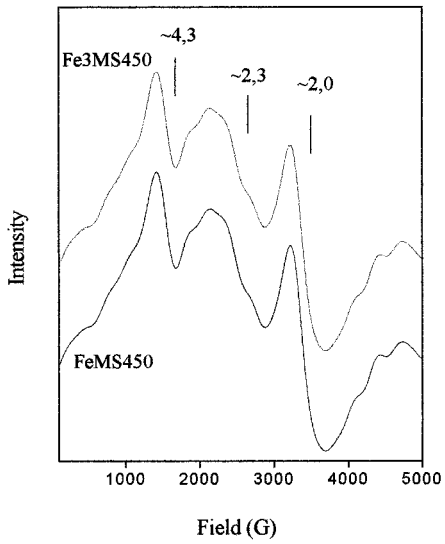

Figure 10. EPR spectra of samples FeMS450 and Fe3MS450 after exposure to acetic anhydride vapors, recorded at 20 K.

After exposure the EPR signals changed drastically (Figure 10). We take that these changes are caused by the penetration and then reaction of the acetic anhydride with the iron centers. These changes constitute strong evidence for the iron accessibility. Finally, in order to establish that iron is grafted to the silicate framework and not simply adsorbed, samples of the iron-planted materials were treated several times with an aqueous LiCl solution. Only traces of Fe^{3+} were detected in the washing solutions.

Conclusions

In the present work we have prepared iron-containing MCM-41 materials, designated as Fe−MCM-41 and Fe3-MCM-41, using an exchange route between the template of the starting material and $FeCl_3$ and $(Fe_3Ac_6O{\cdot}3H_2O)NO_3$. The content of iron in samples FeMS450 and Fe3MS450 was found to be 1.6% and 2.7%, respectively.

The exchange reactions are significantly affected by the network connectivity of the starting material MCM-41. Total removal (93%) and isolation (85%) of the surfactant from the initial solid MCM-41 in the form of a perchlorate salt was realized. Quantitative measurements showed that the template consisted of 33% ion pairs and 67% of ion exchangeable organic phase.

The iron-substituted products obtained before and after calcination at 450 °C showed high crystallinity as indicated by the X-rays diffraction patterns.

The calcined samples FeMS450 and Fe3MS450 possessed high BET surface areas (~1000 m^2 g^{-1}), pore diameters in the class of microporous materials, and increased wall thickness comparing with a MCM-41/450 solid. The last finding indicates iron grafting into the network of the final products. Grafting of iron into the silicon oxide network is supported also by reflectance-IR, EPR, and Mössbauer spectroscopies. Iron is strongly bonded to the inorganic network of the silica and is easily accessible by molecules absorbed onto the pores of the materials.

Acknowledgment. The authors thank Dr. A. Simopoulos for assistance in measuring and discussing the Mössbauer spectra.

References and Notes

(1) Beck, J. S.; Vartuli, J. C.; Roth, W. J.; Leonowicz, M. E.; Kresge, C. T.; Schmitt, K. D.; Chu, C. T−W.; Olson, D. H.; Sheppard, E. W.; McCullen, S. B.; Higgins, J. B.; Schlenker, J. L. *J. Am. Chem. Soc.* **1992**, *114*, 10834.

(2) Raman, N. K.; Anderson, M. T.; Brinker, C. J. *Chem. Mater.* **1996**, *8*, 1682.

(3) Davis, M. E.; Chen, C.-Y.; Burkett, S. L.; Lobo, R. F. *Mater. Res. Soc. Proc.* **1994**, *346*, 831.

(4) Tanev, P. T.; Pinnavaia, T. J. *Chem. Mater.* **1996**, *8*, 2068.

(5) Whitehurst, D. D. U.S. Patent 1992, No. 5,143,879.

(6) Kim, J. M.; Kwak, J. H.; Jun, S.; Ryoo, R. *J. Phys. Chem.* **1995**, *99*, 16742.

(7) Yuan, Z. Y.; Liu, S. Q.; Chen, T. H.; Wang, J. Z.; Li, H. X. *J. Chem. Soc., Chem. Commun.* **1995**, 973.

(8) Tuel, A.; Gontier, S. *Chem. Mater.* **1996**, *8*, 114.

(9) Yang, R. T.; Pinnavaia, T. J.; Li, W.; Zhang, W. *J. Catal.* **1997**, *172*, 488.

(10) Echchahed, B.; Moen, A.; Nicholson, D.; Bonneviot, L. *Chem. Mater.* **1997**, *9*, 1716.

(11) He, N. Y.; Bao, S. L.; Hu, Q. H. *Stud. Surf. Sci. Catal.* **1997**, *105*, 85.

(12) Tuel, A.; Arcon, I.; Millet, J. M. M. *J. Chem. Soc., Faraday Trans.* **1998**, *94*, 3501.

(13) Hitz, S.; Prins, R. *J. Catal.* **1997**, *168*, 194.

(14) Yonemitsu, Y.; Tanaka, Y.; Iwamoto, K. *Chem. Mater.* **1997**, *9*, 2679.

(15) Starke, K. *J. Inorg. Nucl. Chem.* **1960**, *13*, 254.

(16) Anderson, M. T.; Martin, J. E.; Odinek, J.; Newcomer, P. In *Access in Nanoporous Materials*; Pinnavaia, T. J., Thorpe, M. F., Eds.; Plenum Press: New York, 1995, p 29.

(17) Rierce, C. *J. Phys. Chem.* **1953**, *57*, 149.

(18) Gerstl, Z.; Banin, A. *Clays Clay Mineral.* **1980**, *28* (5), 335.

(19) Kamitsos, E. I.; Patsis, A. P.; Kordas, G. *Phys. Rev. B* **1993**, *48*, 12499.

(20) Takano, M. *J. Phys. Soc. Jpn.* **1972**, *33* (5), 1312.

(21) Meagher, A.; Nair, V.; Szostac, R. *Zeolites* **1988**, *8*, 3.

(22) Ratnasamy, P.; Kumar, R. *Catal. Today* **1991**, *9* (4), 329.